GSA Data Repository 2016149

Late Cenozoic surface uplift of the southern Sierra Nevada (California, USA): A paleoclimate perspective on lee-side stable isotope paleoaltimetry

Wheeler et al.

Pre-Industrial and Miocene Simulations

The middle Miocene is thought to be significantly warmer than modern climate (Zachos et al., 2008). We calculated annual averages of precipitation and temperature for both the Miocene and Pre-Industrial (PI) simulations of climate from 50 consecutive years. Results from the simulated Miocene climate show a global increase in temperature of 4.6°C and a global increase in precipitation of 150 mm relative to the PI simulation. The Miocene temperature increase relative to the PI simulation is in line with the 5-6 °C temperature excursion from deep ocean benthic oxygen isotopes for 17-14.5 Ma (Zachos et al., 2008). Temperature and precipitation proxies for western North America suggest that the region was both warmer and wetter than modern climate (White and Auger, 1994; Wolfe 1994a; Wolfe 1994b; Sheldon, 2006; Retallack, 2004). The Miocene simulation captures both an increase in temperature and precipitation for western North America relative to the PI simulation (Fig. DR1, Fig. DR2, Fig. DR3, Fig. DR4).

Simulations of Flow around Idealized Terrain

Using the Weather Research and Forecasting (WRF) model version 3.5.1 (Skamarock et al., 2008) we ran two sets of simulations for various topographic and climatic states to determine how stable a climate is needed in order for the 2D assumptions used in the leeside proxies to faithfully record the elevation of both a high

and low southern Sierra Nevada. The initial conditions for these two simulations are outlined in Table DR1 and Table DR2.

Modern Nh/U Calculation

We calculated N_m from five consecutive years (1995-1999) of 3-hourly North American Regional Reanalysis (NARR) output (http://www.esrl. noaa.gov/psd/). N_m was calculated for the windward region of the Sierra after Durran and Klemp (1982). We find that the average $N_m = 0.0086\ s^{-1}$ with an average modern Nh/U of 2.2. Using the 10^{th} percentile N_m, where $N_m = 0.0071\ s^{-1}$, $Nh/U = 1.8$. For our calculations of Nh/U we use $h = 3$ km.

FIGURE CAPTIONS

Figure DR1. Pre-Industrial simulation annual surface temperatures (°C). The black line is the modern land-ocean boundary.

Figure DR2. Miocene minus the Pre-Industrial simulation annual surface temperature anomaly (°C). Black contour is the Miocene land-ocean boundary.

Figure DR3. Pre-Industrial simulation annual average precipitation (mm). The black line is the modern land-ocean boundary.

Figure DR4. Miocene minus the Pre-Industrial simulation annual precipitation anomalies (mm). Black contour is the Miocene land surface boundary.

Table DR1. Initial conditions for simulations of idealized flow for an idealized high southern Sierra Nevada.

Table DR2. Initial conditions for simulations of idealized flow for a uniform ridge increasing in elevation.

REFERENCES

Gent, P. R. et al., 2011, The Community Climate System Model Version 4, Journal of Climate, v. *24*(19), p. 4973–4991.

Durran, D.R., and Klemp, J.B., 1982, On the Effects of Moisture on the Brunt-Vaisala Frequency: J. Atmos. Sci., v. 39, p. 2152–2158

Retallack, G.J., 2004, Late Miocene climate and life on land in Oregon within a context of Neogene global change: Palaeogeography, Palaeoclimatology, Palaeoecology, v. 214, p. 97–123.

Sheldon, N.D., 2006, Using paleosols of the Picture Gorge Basalt to reconstruct the middle Miocene climatic optimum: PaleoBios, v. 26, p. 27–36.

Skamarock, W.C., Klemp, J.B., Dudhi, J., Gill, D.O., Barker, D.M., Duda, M.G., Huang, X.-Y., Wang, W., and Powers, J.G., 2008, A Description of the Advanced Research WRF Version 3: NCAR Technical Note, v. Tech. Note, p. 113.

White, J. M., and T. A. Ager, 1994: Palynology, paleoclimatology and correlation of Middle Miocene beds from Porcupine River (locality 90-1), Alaska. Quat. Int., 22–23, 43–77.

Wolfe, J. A., 1994a: Tertiary climatic changes at middle latitudes of western North America. Palaeogeogr., Palaeoclimatol., Pa- laeoecol., 108, 195–205.

Wolfe, J. A., 1994b: An analysis of Neogene climates in Beringia. Palaeo- geogr., Palaeoclimatol., Palaeoecol., 108, 207–216.

Zachos, J.C., Dickens, G.R., and Zeebe, R.E., 2008, An early Cenozoic perspective on greenhouse warming and carbon-cycle dynamics.: Nature, v. 451, p. 279–283.

Fig. DR1

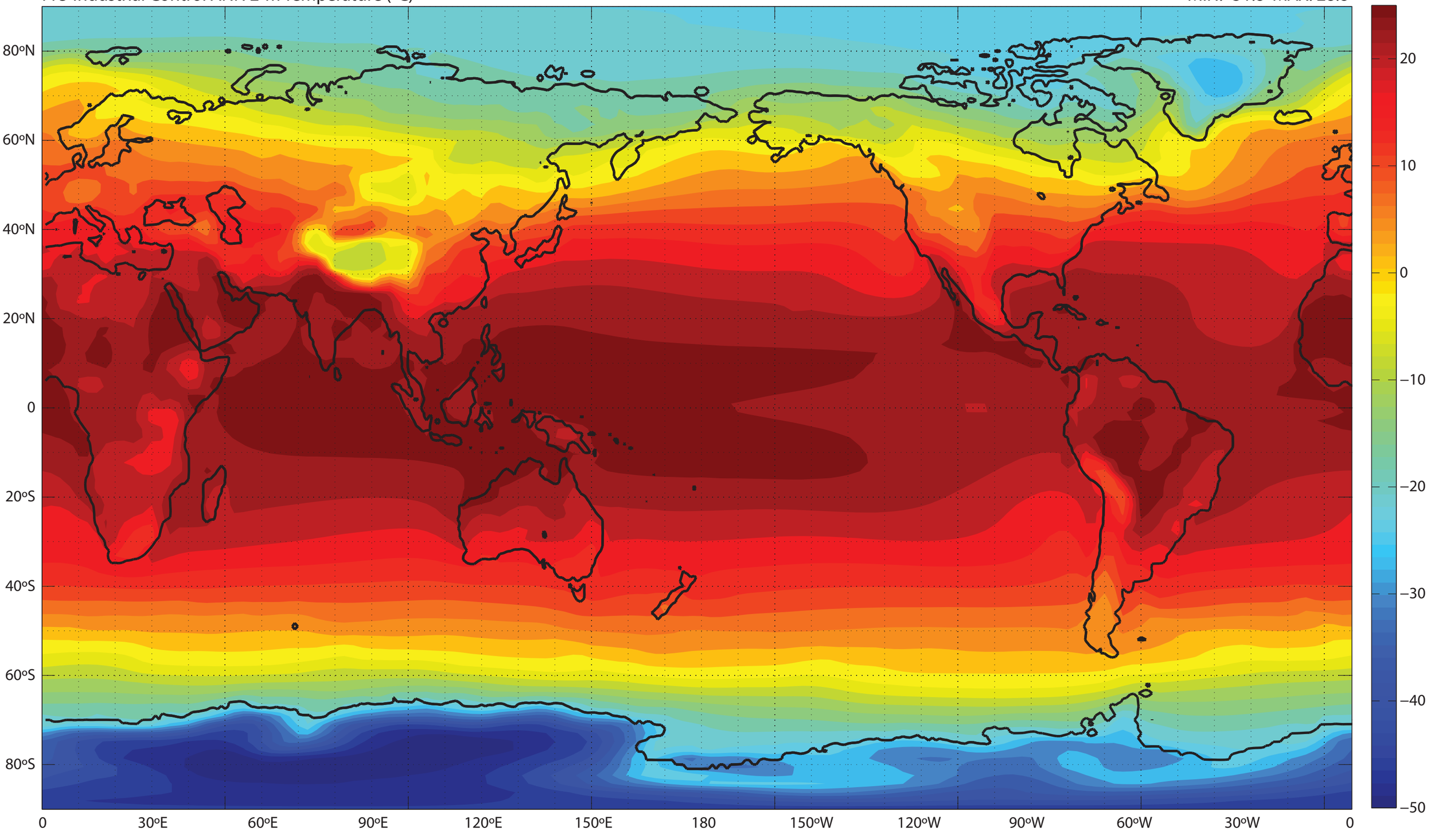
Pre-Industrial Control ANN 2-m Temperature (°C)
MIN: -51.8 MAX: 28.8
80°N
60°N
40°N
20°N
0
20°S
40°S
60°S
80°S
0
30°E
60°E
90°E
120°E
150°E
180
150°W
120°W
90°W
60°W
30°W
0
20
10
0
−10
−20
−30
−40
−50

Fig. DR2

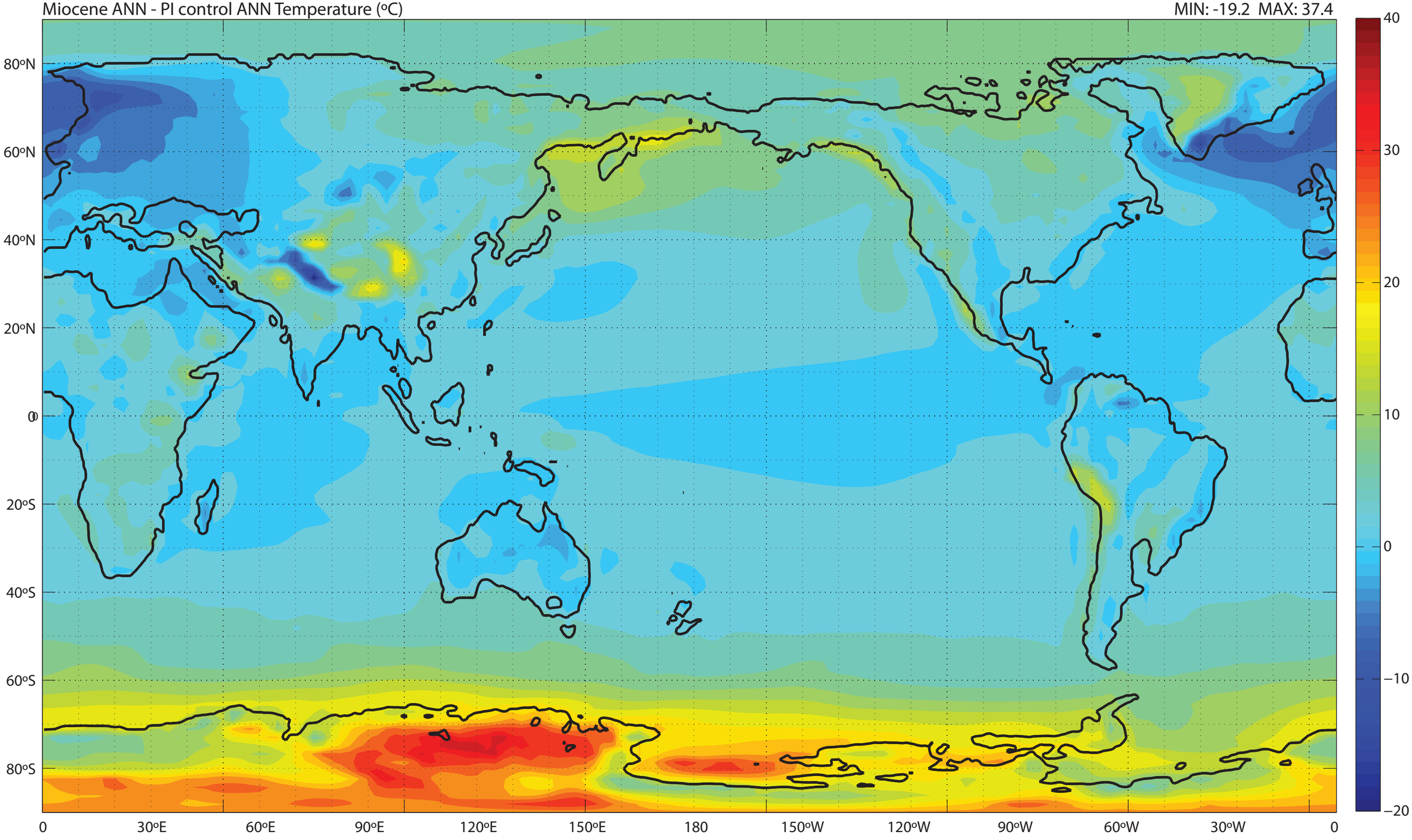
Miocene ANN - PI control ANN Temperature (°C)
MIN: -19.2 MAX: 37.4
80°N
60°N
40°N
20°N
0
20°S
40°S
60°S
80°S
0
30°E
60°E
90°E
120°E
150°E
180
150°W
120°W
90°W
60°W
30°W
0
40
30
20
10
0
−10
−20

Fig. DR3

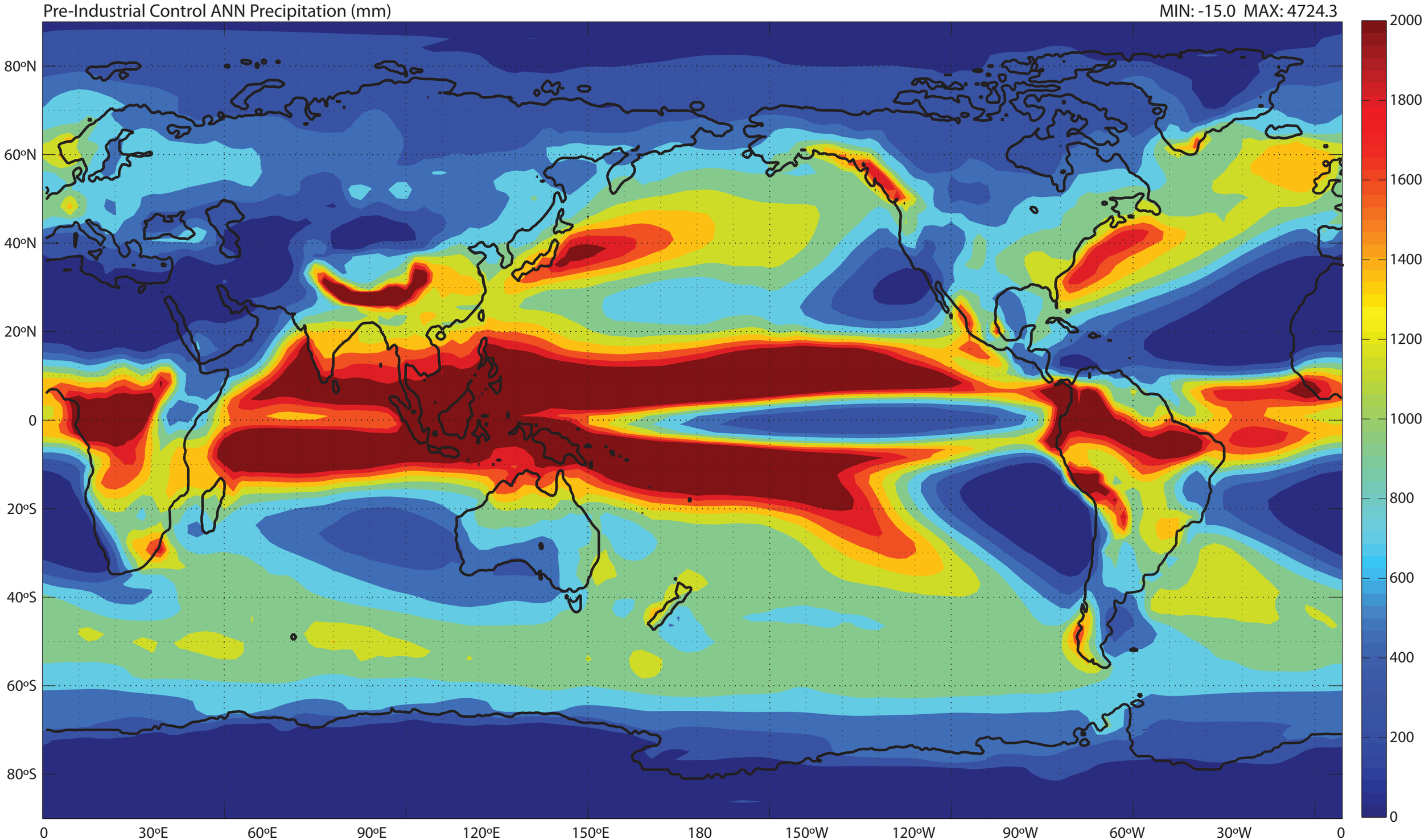
Pre-Industrial Control ANN Precipitation (mm)
MIN: -15.0 MAX: 4724.3
80°N
60°N
40°N
20°N
0
20°S
40°S
60°S
80°S
0
30°E
60°E
90°E
120°E
150°E
180
150°W
120°W
90°W
60°W
30°W
0
2000
1800
1600
1400
1200
1000
800
600
400
200
0

Fig. DR4

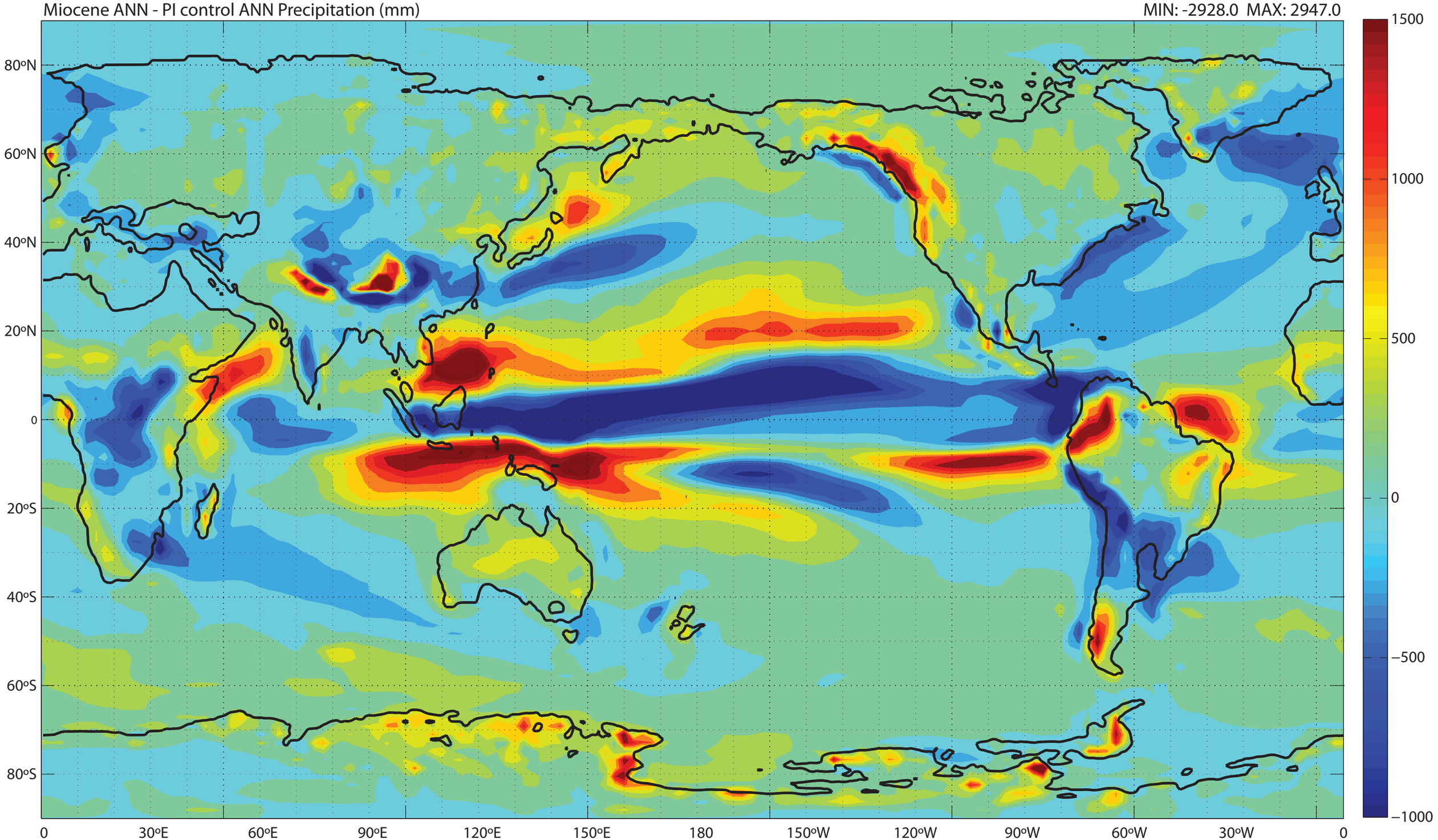
Miocene ANN - PI control ANN Precipitation (mm)
MIN: -2928.0 MAX: 2947.0
80°N
60°N
40°N
20°N
0
20°S
40°S
60°S
80°S
0
30°E
60°E
90°E
120°E
150°E
180
150°W
120°W
90°W
60°W
30°W
0
1500
1000
500
0
−500
−1000

Table DR1

Experiment	Brunt-Vaisala frequency (1/s)	Nh/U
High_SSN_01	0.0025	0.80
High_SSN_02	0.0038	1.10
High_SSN_03	0.0049	1.50
High_SSN_04	0.0058	1.75
High_SSN_05	0.0061	1.80
High_SSN_06	0.0075	2.30
High_SSN_07	0.01	3.00

Table DR2

Experiment	Brunt-Vaisala frequency (1/s)	Maximum Ridge Height (m)
LowRidge_01	0.0032	500
LowRidge_02	0.0032	1000
LowRidge_03	0.0032	1500
LowRidge_04	0.0032	2000
LowRidge_05	0.0032	2500
LowRidge_06	0.0032	3000
LowRidge_07	0.0032	3500
LowRidge_08	0.0075	2000